4-1-1961

Analysis of scintillation pulse shapes for stilbene using neutron and gamma-ray excitation

Roland Lee Bowles

Bowles

42

ANALYSIS OF SCINTILLATION PULSE SHAPES FOR STILBENE USING NEUTRON AND GAMMA-RAY EXCITATION

by

ROLAND LEE BOWLES

A thesis submitted to the Faculty of
the University of Richmond in partial
fulfillment of the requirements for
the degree of Master of Science in
the Department of Physics

Richmond, Virginia

1961

Addison H. Compton
Jackson J. Taylor
Billy A. Cooper
Charles B. Hurd
Francis B. Kay
Wilton R. Tenney

II. TABLE OF CONTENTS

III. LIST OF FIGURES

IV. INTRODUCTION

In experimental nuclear physics it is often desirable to detect neutrons in the presence of a heavy gamma-ray background. This situation presents a problem since neutron counters also respond to gamma radiation. However, recently it has been shown that the scintillation counter employing an organic crystal scintillator and pulse-shape discrimination may well furnish the solution to this problem.

Neutrons can be counted with organic scintillators through the detection of the scintillations produced by protons recoiling from neutron-proton collisions within the crystal. On the other hand gamma-rays manifest themselves in the crystal through the fast electrons they produce. However, it is well known that the light output from an organic scintillator for fast, heavy particles (recoiling protons) is much less than for electrons of equal energy. The maximum pulse height produced by a proton of 2 Mev energy entering an anthracene crystal is only 2/5 of that produced by an electron of the same energy[1]. Therefore, the pulse heights due to fast neutrons are appreciably smaller than those due to gamma-rays of the same energy, thus making the detection of neutrons in the presence of γ-rays very difficult. Currently much effort is being expended in the development of neutron sensitive scintillators whose efficiency for the detection of gamma-rays is considerably reduced.

Even though the solid organic neutron detector has the above disadvantages, it also has some very definite advantages. This type counter has a high detection efficiency. Second, it has a very fast response to incident radiation. An organic scintillator such as stilbene or anthracene has a response time of 10-20 $m\mu$ sec[2].

The fact that there exists a difference in the decay times of scintillation pulses produced by electrons and protons in organic phosphors suggests the possibility of using this phenomenon to distinguish between neutrons and γ-rays. Methods of overcoming gamma-ray sensitivity has been developed by F. D. Brooks[3] following the work of G. T. Wright[4]. Wright[4] has shown that the charge pulse at the anode of the photomultiplier tube used in conjunction with an anthracene crystal has decay times of 31 mμ sec and 53 mμ sec for electron and alpha particle excitation, respectively. It was also reported by Brooks[5] and Owens[6] that other organic phosphors such as stilbene, naphtalene, quaterphenyl, and properly de-oxygenated liquids showed similar properties.

As a result of this work, it can be concluded that decay times are effectively larger for heavier, more highly ionizing particles, such as protons, than for electrons. The above findings suggest the possibility of identifying the particles producing scintillations in organic phosphors. This effect has recently been employed in a new type of scintillation counter which will discriminate efficiently between protons, alpha-particles and electrons. Brooks[5] has developed a counter which distinguishes fast neutrons from gamma rays by utilizing the effective decay time differences between the pulses produced by recoil protons and electrons. The circuit used by Brooks[5] enables one to balance out all pulses associated with one effective decay time, but to detect and count those which have a larger decay time. Owens[6] also developed several circuits which have the ability to identify the type of incident radiation. H. W. Broeks and C. E. Anderson[7], and H. O. Funsten[8], employing circuits similar to those used by Owens[6], have successfully made particle identification.

Detailed analysis of these circuits used can be found in reference 6. A careful survey of the work being done in this field indicates that stilbene is the most promising of the organic scintillators for purposes of particle identification.

Since a definite difference exists in the light pulse emitted by an organic phosphor when excited by particles of different specific ionization, it was decided to develop a mathematical model which would predict the observed pulse shape differences and thus provide information for the design of a circuit which will efficiently discriminate between neutrons and gamma-rays. (Stilbene was used as the scintillator in this model.) Hence, it was decided to study the pulse shape as a function of time.

Scintillation pulse shapes have been studied by Owens[6], Swank[7], Harrison[10], Wright[4], Birks[11], Kallman and Brucker[12]. From a careful survey of their data one might conclude that for organic scintillators the most general scintillation decay pulse may be described as a sum of several exponential components. The first component can be described as a "fast" millimicrosecond component which carries 80 percent or more of the total light in the scintillation. In addition to this component there also exists one or more "slow" components which have decay times between 0.1 μsec and 100 μsec. Harrison[10] showed that pulses produced in anthracene and stilbene contained several slow components, the decay times for stilbene ranging from .25 μsec to 80 μsec. He also showed that liquid scintillators produce few, if any, slow components. Kallman and Brucker[12] concluded that there is essentially no difference in the "fast" decay time for electron and alpha excitation. This finding was verified for a large

number of organic solids and liquids. Owens[6] also showed that the fast component decay times were not influenced by particles of different specific ionization. He also was able to show that the "slow" component decay times were the same for electron and proton excitation in a wide variety of phosphors. However, the number of slow component emissions was higher, and that of fast component lower, in proton scintillations. In fact, the longer lived components were found to be about twice as intense under proton excitation as under gamma-ray or electron excitation. Thus, the net or composite decay time for protons is considerably longer than that for electrons because proton scintillations contain a higher number of slow components.

In order to interpret the effective decay time difference of stilbene, consider a proton or electron stopping in the crystal. The incident particle loses energy dE in an element of distance dX along its track by producing excited molecules M^* and ionized molecules M^+. There are primarily two modes by which the excited molecules decay.

These are:

$$M^* \rightarrow M + h\nu \qquad (1)$$

$$M^* \rightarrow M + \text{heat energy} \qquad (2)$$

In the first process the molecule emits light photons which could ultimately be detected. The second process is a quenching process where electronic excitation energy is converted into vibrational energy. Ionized molecules formed by the incident particle must undergo a delayed recombination process,

$$M^+ + \bar{e} \rightarrow M^{*'} \qquad (3)$$

The excited molecule M^* formed by recombination can now decay by either (1) or (2). It has been suggested that the recombination process is relatively slow, having a lifetime of approximately 10^{-7} sec[5]. According to Birks, the light output is a function of the initial ionization and excitation density i.e. number of M^+ and M^* per unit path length along the track in the scintillator. For proton excitation, where the ionization and excitation density is high, the excited molecules find themselves in an environment which offers additional modes of quenching. Thus, for protons, less light is emitted initially (fast components) than for electrons which have a considerably smaller ionization and excitation density. Near the end of the path where dE/dX is greatest, more M^+ molecules are formed and hence recombine according to (3). However, M^* molecules are born into an environment where the excitation density is much less than it was initially so the molecules are most likely to emit photons rather than be quenched. This slow component decay time is essentially the recombination time. Thus for heavily ionizing protons more light would be emitted in the long component than for electrons.

In this discussion photon emission from stilbene crystals is assumed to be composed of K exponential components. The charge pulse appearing at the anode of the photo-multiplier is determined analytically, by studying the time dependence of the associated voltage pulse. Using the assumed model for scintillation decay, a method is devised which enables one to calculate the decay times of the components involved. As a result of this model the percentage light carried by each component is determined, thus checking the conclusions of Owens[6]. The analytical shape of the charge pulse appearing at the anode is compared to the observed pulse

shapes. The experimental results were obtained by using the assumed model as a guide. An expression is given for a dimensionless variable which completely describes the pulse shape. This variable is normalized to the peak pulse height and is a direct result of the assumed model. A correlation is made between the observed pulse shapes and those predicted by the assumed model, hence justifying the initial assumptions. The pulse shapes were observed under neutron and gamma-ray excitation. Therefore, conclusions can be made as to the variation of charge pulse shapes for particles of different specific ionization.

V. THEORY

The voltage pulse appearing at the anode of a photo-multiplier tube, due to a scintillation, will be analytically described in terms of the circuitry shown in figure 1. The photomultiplier is connected and used in the conventional manner. Let C_s denote the total stray capacitance shunting the anode load resistor R_1.

The equivalent A. C. circuit of the output stage of the multiplier tube is given in figure 2. In this analysis, it is assumed that the input impedance of the oscilloscope is purely resistive. Also shown in figure 2 is a block diagram of the individual circuit elements which will effect the voltage pulse $E(t)$. In each block the transfer function relating the input and output variables for that particular block is shown. The transfer functions are written in usual operator notation, where $P = \frac{d}{dt}$ is a complex differential operator. From figure 2 it can be seen that

$$\frac{eo(t)}{i(t)} = \frac{R_1}{(\tau o)_1 P + 1} \tag{1}$$

where $(\tau o)_1 = (C_s + C_1)R_1$ is the anode time constant. Likewise:

$$\frac{E(t)}{eo(t)} = \frac{(\tau o)_2 P}{(\tau o)_2 P + 1} \tag{2}$$

where $(\tau o)_2 = R_2 C_2$ is the input time constant of the measuring circuit (oscilloscope). By combining equations (1) and (2) we can relate $E(t)$ to $i(t)$,

$$\frac{E(t)}{i(t)} = \frac{R_1 (\tau o)_2 P}{\left[(\tau o)_2 P + 1\right]\left[(\tau o)_1 P + 1\right]} \tag{3}$$

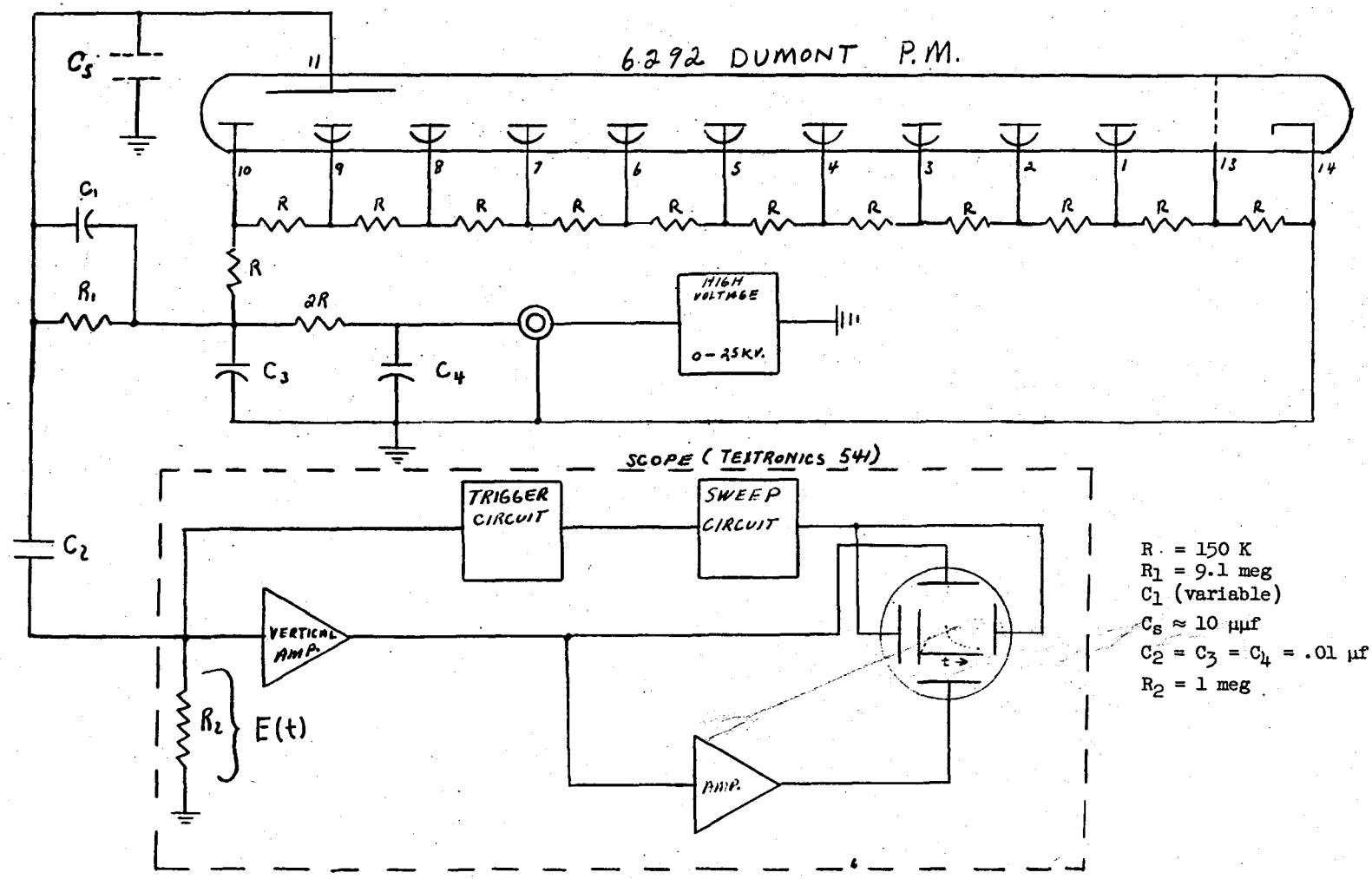

Figure 1.- Photomultiplier and associated circuits.

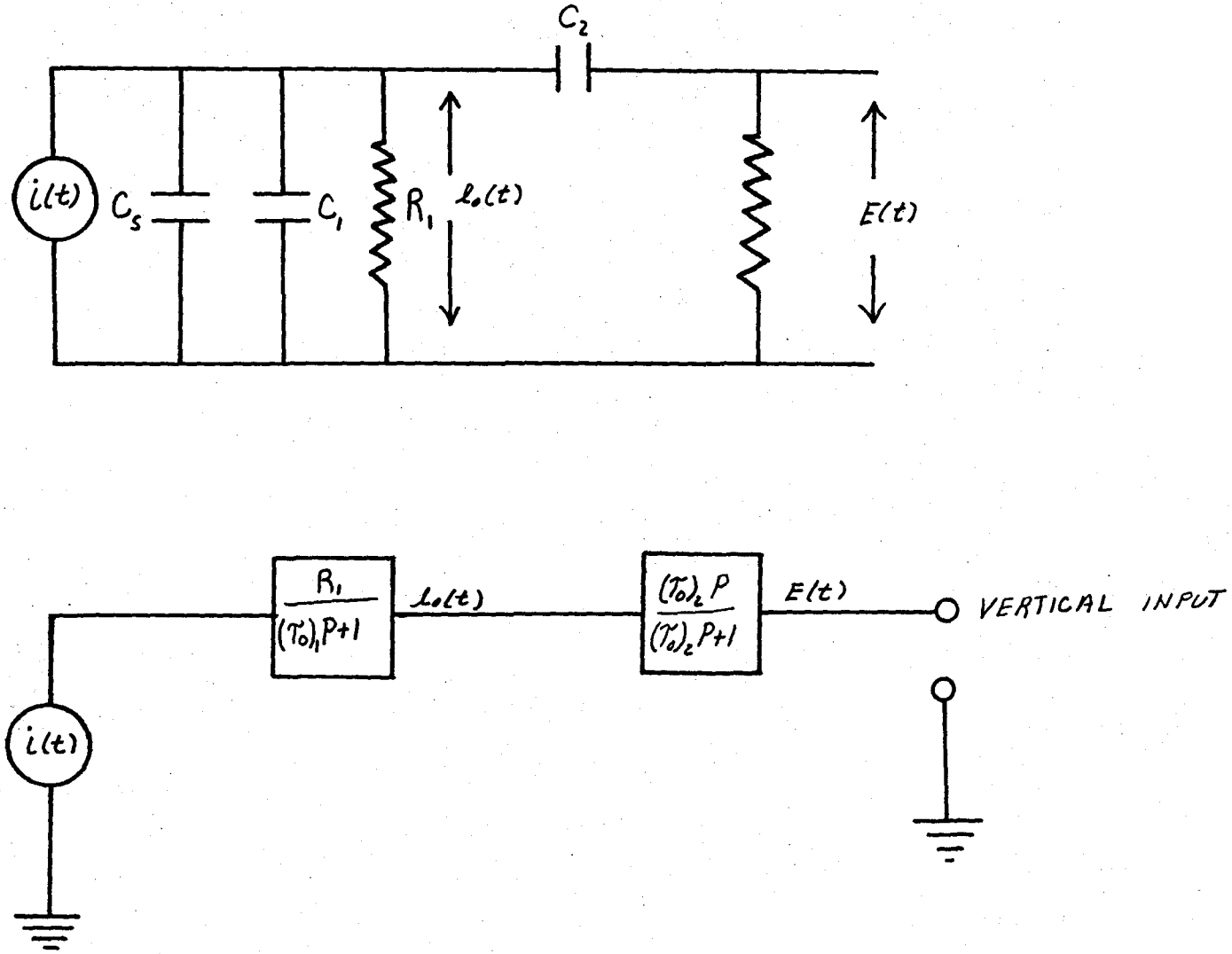

Figure 2.- Equivalent A.C. circuit.

Expanding the denominator of the above equation and making the assumption that $(\tau_o)_2 \gg (\tau_o)_1$ and $P \gg 1$ we obtain:

$$\frac{E(t)}{i(t)} = \frac{R_1(\tau_o)_2 P}{(\tau_o)_2(\tau_o)_1 P^2 + \left[(\tau_o)_1 + (\tau_o)_2\right] P + 1}$$

$$= \frac{R_1}{(\tau_o)_1 P + 1} \tag{4}$$

The above results indicate that the anode circuit can be considered as consisting of only a resistance and capacitor in parallel, if the assumption $(\tau_o)_2 \gg (\tau_o)_1$ is made and if the input of the scope is only resistive. This result will enable us to describe the voltage pulse by a first order differential equation. Thus, we have shown that the pulse shape is independent of the C_2 and is determined only by $(\tau_o)_1$ and the analytical form of i(t), where i(t) is the current pulse at the anode of the multiplier tube resulting from a scintillation.

In order to describe the operation of the circuit, consider the effective load at the anode of the multiplier to consist of a capacitance, $C_s + C_1$, in parallel with a resistance R_1. It follows from equation (4) that the differential equation describing the voltage pulse at the anode can be given by

$$(C_s + C_1)\frac{dE}{dt} + \frac{E}{R} = i(t) \tag{5}$$

for $0 \leq t \leq t_o$ and i(t) non-zero, where t_o is the time required for the voltage pulse to reach its maximum value E_o. For $t_o \leq t \leq \infty$, $i(t) = 0$ so the voltage pulse can be described by

$$(C_s + C_1)\frac{dE}{dt} + \frac{E}{R} = 0 \tag{6}$$

Rewriting equations (5) and (6) in terms of $(\tau_o)_1$ we obtain

$$\frac{dE}{dt} + \frac{E}{\tau_o} = \left[\frac{1}{C_s + C_1}\right] i(t) \qquad 0 \leq t \leq t_o \tag{7}$$

and

$$\frac{dE}{dt} + \frac{E}{\tau_o} \equiv 0 \qquad t_o \leq t \leq \infty \tag{8}$$

where

$$\tau_o = (\tau_o)_1 = (C_s + C_1)R_1.$$

The initial conditions which must be satisfied in order to completely describe the pulse shape are

$$E(0) = o, \quad E(t_o) = E_o \quad \text{and} \quad E(t = \infty) = 0$$

The solution of equations (7) and (8) using the initial conditions given above will completely describe the voltage pulse as a function of time, assuming $i(t)$ to be a known function. In the above analysis, $i(t)$ is a function which is dependent on the properties of the particular scintillator used. In the forthcoming development we will assume an appropriate form for $i(t)$ and thus obtain a solution to equations (7) and (8).

Assume that the stilbene crystal is excited at $t = o$ by a high energy ionizing particle. Let us further assume that the photon emission by the phosphor when it de-excites is composed of K independent components of light. The fraction of fluorescence photons emitted between t and $t + dt$, compared to total number N_o emitted in the scintillation, can be given by

$$\frac{dN(t)}{\sum_{K=1}^{l} N_K} = \sum_{K=1}^{l} f_k(t)dt \tag{9}$$

where N_k is the number of photons emitted in the Kth components and

$$\sum_{K=1}^{l} N_k = N_o.$$

It follows that the rate of photon emission for $t > 0$ is

$$\frac{d}{dt} N(t) = \sum_{K=1}^{l} N_k \sum_{K=1}^{l} f_k(t) = \sum_{K=1}^{l} N_k f_k(t) \tag{10}$$

We shall assume that $f_k(t)$ is a step rise followed by an exponential decay, since photon emission is a first order process. Thus $f_k(t)$ assumes the following form

$$f_k(t) = \frac{e^{-t/\tau_k}}{\tau_k} \tag{11}$$

and the rate of photon emission for $t > 0$ can be given by

$$\frac{d}{dt} N(t) = \sum_{K=1}^{l} \frac{N_k e^{-t/\tau_k}}{\tau_k} \tag{12}$$

Hence, we have taken the scintillation pulse to be a step rise followed by a series of exponentially decaying components.

The charge which is collected at the anode due to a scintillation can be given by

$$q(t) = \left\{ g\bar{n}(\lambda)\epsilon\bar{s}^{r} \right\} \sum_{K=1}^{l} N_k e^{-\frac{(t-\tau_L)}{\tau_k}} \tag{13}$$

where g is the number of photons/scintillation which falls on the photo-cathode, $\bar{n}(\lambda)$ is the average quantum efficiency for photo-electric conversion at the cathode and is a function of wavelength, λ, of the emitted spectrum. The quantity $\bar{s}^{r}$ is the total gain of the

multiplier tube, where the tube contains r uniform dynode stages each of mean gain $\bar{s}$, and ϵ is the electronic charge. Due to a finite time lag, τ_L, in the multiplier, the anode charge pulse does not necessarily follow the scintillation pulse shape. The net effect of this delay is to shift the maximum value of the charge from $t = o$ to a later point in time. From an inspection of equation (13), one can see that $i(t)$ will have a maximum at $t = \tau_L$ and hence differs from the step rise assumed for the scintillation pulse. By operating the multiplier at large values of plate voltage, τ_L can be minimized to some extent. In general $\tau_L \approx 10^{-10}$ sec which is an order of magnitude smaller than τ_k for most scintillators. The anode current can now be given by

$$i(t) = \frac{d}{dt}\left[q(t)\right] = \left\{g\bar{n}(\lambda)\epsilon\bar{s}^r\right\}\sum_{K=1}^{l}\frac{N_k}{\tau_k}e^{-t/\tau_k+\delta_k} \tag{14}$$

where

$$\delta_k = \tau_L/\tau_k.$$

Substituting the above value of $i(t)$ into equation (7) one obtains

$$\frac{dE}{dt} + \frac{E}{\tau_o} = \frac{\phi}{C_s + C_l}\sum_{K=1}^{l}\frac{N_k}{\tau_k}e^{-t/\tau_k+\delta_k} \qquad 0 \le t \le t_o \tag{15}$$

where $\phi = g\bar{n}(\lambda)\epsilon\bar{s}^r$ is assumed to be invariant. Equation (15) is a first order, linear differential equation which can be solved by applying the integrating factor e^{+t/τ_o}. The solution of the above equation is of the following form, where the constant of integration is determined by applying the initial condition $E(0) = 0$.

$$E(t) = \frac{\phi}{C_s + C_1}\sum_{K=1}^{l}\frac{N_k}{\tau_k}\left(\frac{\tau_k\tau_o}{\tau_o - \tau_k}\right)e^{\delta_k}\left(e^{-t/\tau_o} - e^{-t/\tau_k}\right)_1 \qquad (16)$$

The solution for equation (8) for $t > t_o$ is given by

$$E(t) = \frac{\phi}{C_s + C_1}\sum_{K=1}^{l} N_k e^{\delta_k} e^{-t/\tau_o} \qquad t \geq t_o \qquad (17)$$

The above two equations describe the voltage pulse at the anode at a time t after the scintillation is produced. Here $\phi N_k = q_k$ is the charge collected by the anode due to the Kth component and $\sum_{K=1}^{l} q_k = q_o$ is the net total charge which flows to the anode during the whole scintillation. The voltage pulse depends not only on τ_k (decay parameter of the scintillator) but also on q_k, and τ_o. It is desirable to eliminate the dependence of $E(t)$ on the parameter τ_o, and hence obtain a clearer picture of how $E(t)$ varies as a function of τ_k, q_k and time. Rewriting equation (16) and using the definition of q_k, one obtains

$$E(t) = \frac{1}{C_s + C_1}\sum_{K=1}^{l}\frac{q_k\tau_o}{\tau_o - \tau_k}e^{\delta_k}\left(e^{-t/\tau_o} - e^{-t/\tau_k}\right).$$

If $\tau_o \gg \tau_k$ the above equation reduces to:

$$E(t) = \frac{1}{C_s + C_1}\sum_{K=1}^{l} q_k e^{\delta_k}\left(1 - e^{-t/\tau_k}\right) \qquad (18)$$

The derivative of equation (18) is given by:

$$\frac{dE(t)}{dt} = \frac{1}{C_s + C_1}\sum_{K=1}^{l}\frac{q_k}{\tau_k}e^{-t/\tau_k + \delta_k} \qquad 0 \leq t \leq t_o \qquad (19)$$

Equation (19) can be rewritten in the following form

$$\left(C_s + C_1\right)\frac{dE(t)}{dt} = i(t) \qquad (20)$$

where $i(t)$ is given by:

$$i(t) = \sum_{K=1}^{l} \frac{q_k}{\tau_k} e^{-t/\tau_k + \delta_k} \qquad 0 \leq t \leq t_o \qquad (21)$$

Thus we obtain a very important result, namely, for $\tau_o \gg \tau_k$, $E(t)$ is proportional to the time integral of $i(t)$.

It can be seen that equations (18) and (20) completely describe the leading edge of the voltage pulse. The leading edge is a function only of q_k, τ_k and time, and is completely independent of τ_o, assuming $\tau_o \gg \tau_k$. The current pulse produces across the R C load a voltage pulse having an exponential rise with time constants equal to those of the K scintillation components. Thereafter, for $t > t_o$, the voltage pulse slowly decays to zero, the rate of decay being determined by the anode circuit time constant, τ_o. This voltage decay is given by equation (17). The leading edge of the voltage pulse contains much useful information concerning the decay properties of the particular phosphor used. For example, if $E(t)$ can be determined experimentally, then $\frac{dE(t)}{dt}$ could be determined graphically and, using equation (20), τ_k and q_k could be calculated. However, this usually is a very difficult procedure to follow and the accuracy with which τ_k and q_k could be determined would be limited considerably.

In order to reduce equation (19) and (20) to a more useable form, we define a dimensionless variable $\gamma(t)$, where: $\gamma(t) = 1 - \frac{E(t)}{E_o}$

of τ_k, q_k and q_k/q_{k+1}, the later parameter being very important when analyzing pulse shapes due to particles of different specific ionization. The function $\gamma(t)$ completely describes the scintillation pulse if δ_k is very small, i.e. a step rise followed by exponentially decaying components. The assumption that $\delta_k \approx 0$ is not a bad one if the photo-multiplier is operated at maximum plate voltage.

Furthermore, an expression relating $\gamma(t)$ and $i(t)$ can be obtained from equation 24. A useful extension of the above equation can be obtained by relating $\gamma(t)$ to $i(t)$

$$\frac{d\gamma(t)}{dt} = -\frac{dE(t)}{dt} \cdot \frac{1}{E_o}$$

$$= -\frac{1}{E_o}\left\{\frac{1}{C_s + C_1}\right\} i(t) \qquad \tau_o \gg \tau_k \quad (25)$$

$$\therefore \qquad \gamma(t^*) - \gamma(0) = -\frac{1}{q_o}\int_0^{t^*} i(t)dt \qquad (26)$$

Thus, if $\delta_k \approx 0$ then $q_o = (C_s + C_1)E_o$ and $\gamma(0) = 1.0$ therefore,

$$\gamma(t^*) = 1 - \frac{1}{q_o}\int_0^{t^*} i(t)dt \qquad 0 \le t \le t_o \qquad (27)$$

Given a known form of $i(t)$, then the normalized charge pulse shape will be completely described by the above integral, assuming exponential decay of scintillation light pulse. Since $\gamma(t)$ is normalized, any variations in photo-multiplier gain or any fluxuations in supply voltage will not effect the normalized pulse shape assuming the tube to a linear component.

VI. EXPERIMENTAL

The purpose of this section is to provide a detailed description of the procedure used in experimentally determining scintillation pulse shapes. Using the assumed mathematical model as a guide, the experimental data is reduced to a form which can be used to formulate pulse shapes. Pulse shapes were determined for a stilbene crystal using neutron and gamma-ray excitation.

The circuit used to determine scintillation pulse shapes is shown in figure 1. The 6292 Dumont photo-multiplier tube was operated with an anode voltage of 1450 volts, thus obtaining 105 volts/dynode. With these voltages the overall gain of the tube is approximately 10^7. This relatively high voltage reduces the electron transit time (τ_L) and the statistical spread of the output voltage pulse. The stilbene crystal ($C_{14}H_{12}$) was mounted on the flat photo-cathode, and the entire crystal-tube assembly was made light tight. Precaution was taken to keep the photo-multiplier tube moderately cool, thus reducing dark noise. Noise due to 60 cycle pick-up was reduced by eliminating all ground loops formed by the photo-multiplier tube and associated circuits. Any auxiliary electronic equipment used was connected to a common high quality earth ground.

The pulse formed at the anode of the multiplier tube was fed to the vertical input of a Textronics model 541 oscilloscope (Fig. 1). The vertical input signal was used to trigger the horizontal sweep circuit, thus providing a time base. This signal was delayed 10 μsec before being passed to the deflection plates. With this arrangement the horizontal

sweep circuit is triggered 10 μsec before the arrival of the vertical input signal at the deflection plates, thus reducing the overall rise time of the scope. The type 541 scope has a .12 mμsec vertical rise time. The display pattern on the cathode ray tube was modulated using the vertical input signal to gate cathode ray tube. The type 541 scope is internally wired to perform the above function. The scope was adjusted to trigger on negative slopes of the input pulses and the triggering level was set at zero volts. The vertical input was calibrated using square waves of known amplitude, and through out this entire experiment the horizontal sweep sensitivity was maintained at .2 μsec/cm. The wave form displayed on the screen of the scope is a plot of E(t) versus t (Fig. 1). These pulses were recorded using a Land Polaroid camera with a special scope attachment. Polaroid type 3000 film was used. This is an extremely fast film and it proved adequate for this application. Enlargements (5" x 8") were made from the original photographs, and these, in turn, were projected on a screen and enlarged by a factor of 2, thus enabling one to analyze them with reasonable accuracy. Photographs of E(t) versus t due to individual scintillation pulses produced by gammy-ray and neutron excitation were obtained. Using Co^{60} as a gamma-ray source, anode voltage pulses were obtained for three values of the anode time constant, τ_o. Only the largest pulses were photographed, these corresponding to the absorption of the 1.17 mev and 1.33 mev gammas emitted by Co^{60}. Use of this relatively high energy excitation helps to reduce statistical variation in pulse shapes. The anode load resistor was taken to be 9.1×10^6 ohms, and two different values of C_1 were used. The stray capacity, C_s, shunting the anode load was determined to be approximately 10 μμf. Values of time constants used are tabulated below, where

$\tau_o = (C_s + C_1) R_1$.

	R_1	C_s	C_1	τ_o
(1)	$9.1 \times 10^6 \Omega$	10 μμf	0	91 μsec
(2)	$9.1 \times 10^6 \Omega$	10 μμf	24 μμf	310 μsec
(3)	$9.1 \times 10^6 \Omega$	10 μμf	40 μμf	455 μ sec

It was found that the leading edge of the voltage pulse was independent of the value of τ_o. This result is in agreement with equation (18), since the three values of τ_o used are extremely large compared to any τ_k encountered for this particular crystal. Figures (3), (4) and (5) illustrate the leading edge of E(t) versus t for three pulses of equal pulse heights, and for anode time constants of 91 μsec, 310 μsec and 455 μsec respectively.

Voltage pulses due to individual scintillations produced by fast neutrons were obtained using a radium-beryllium neutron source. Since this source had a relatively high gamma output, steel blocks were used to shield the scintillation detector from the source. In stilbene, Co^{60} gamma-rays will produce secondary electrons with energies up to about 1.33 Mev. The largest number of neutrons from a radium-beryllium source are emitted at approximately 4.5 Mev and hence provide recoil protons with energies up to 4.5 Mev. Since the luminescent efficiency of stilbene for protons is about 1/3 of that for electrons, the largest of the gamma-ray pulses relative to the most frequent recoil proton pulses is in the ratio of 3(1.33)/4.5. Using only the neutron pulses which occurred most frequently, the peak pulse heights for the neutrons and the 1.33 Mev gammas were very nearly equal, thus reducing nonlinear effects of the crystal and photo-multiplier. A typical voltage pulse obtained

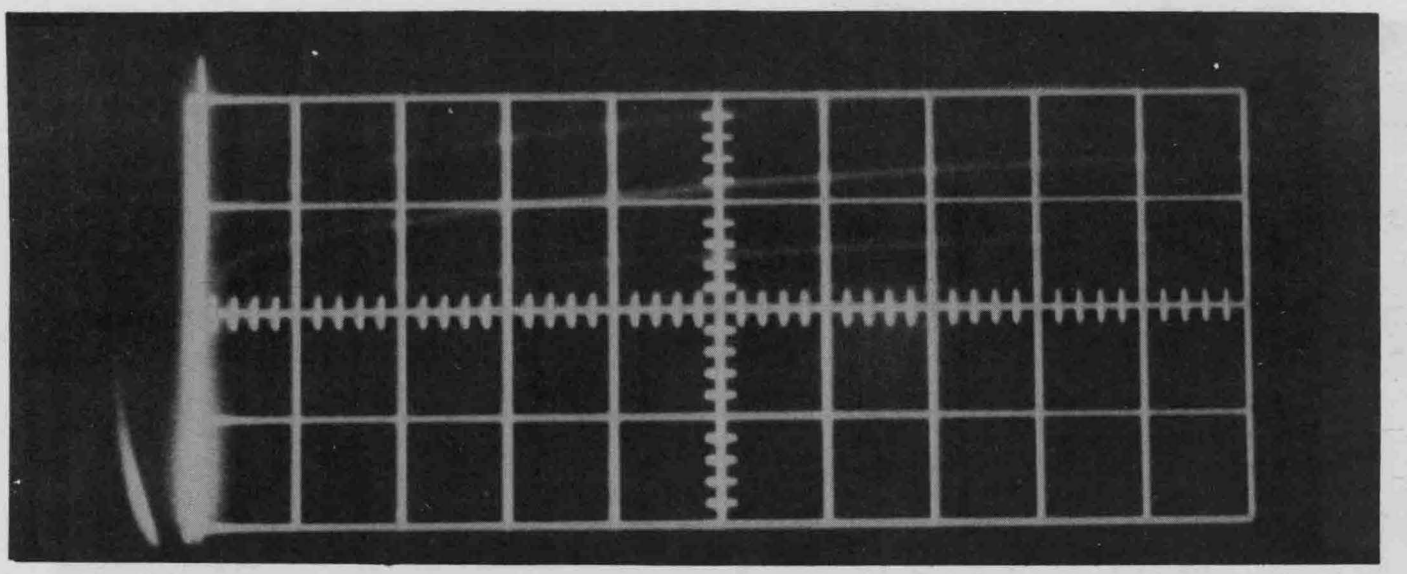

E(t) versus t $(0 \leq t < t_o)$. L-61-2187

Figure 3.- Leading edge of gamma pulse (τ_o = 91 μsec).

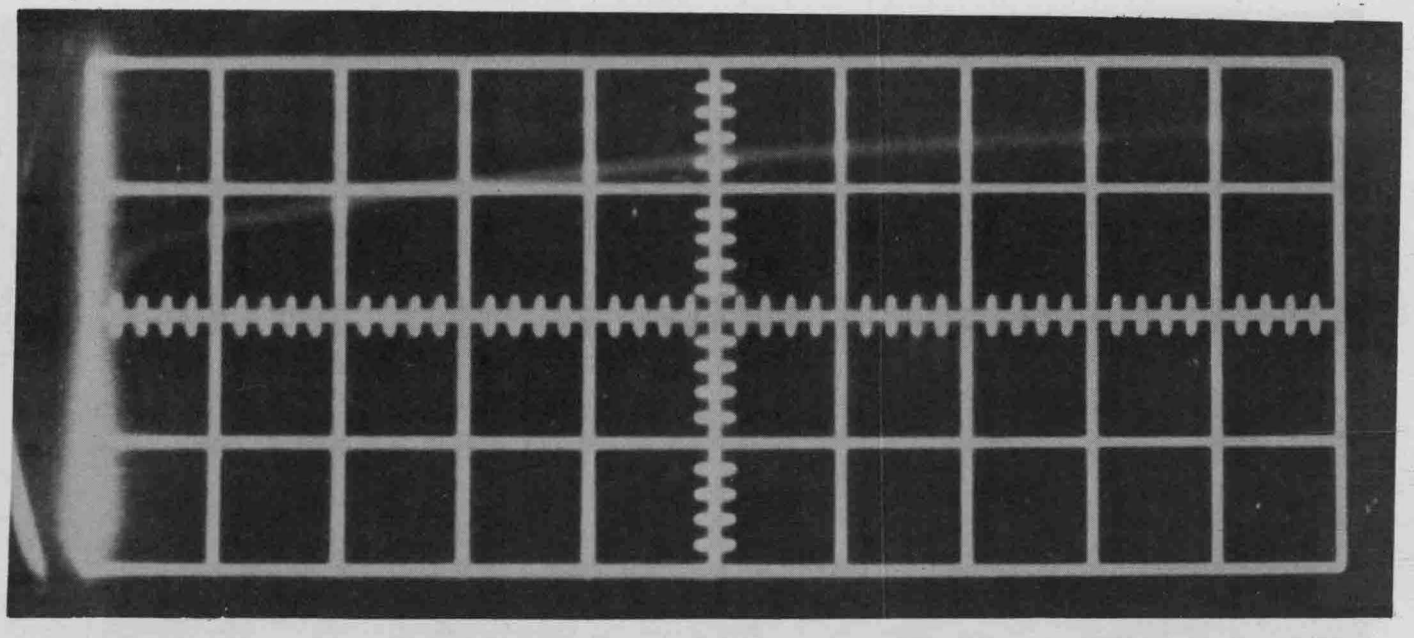

E(t) versus t $(0 \leq t < t_o)$. L-61-2188

Figure 4.- Leading edge of gamma pulse (τ_o = 310 μsec).

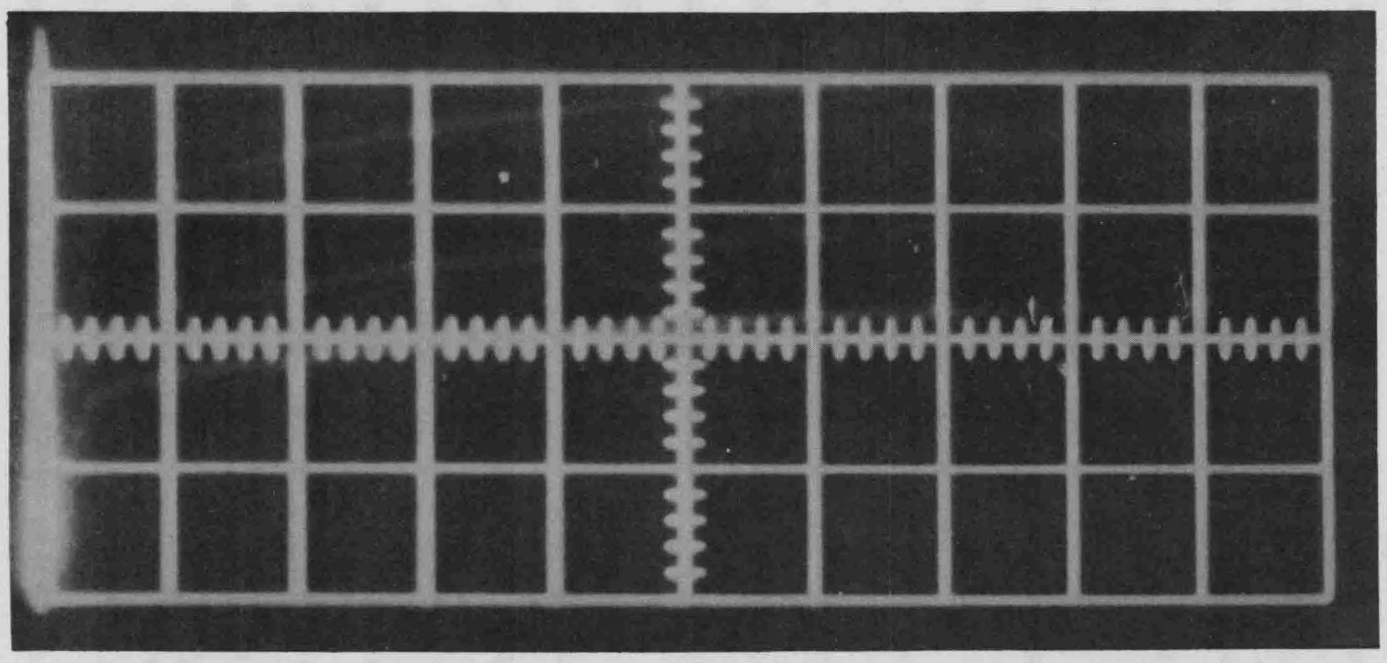

$E(t)$ versus t $\quad (0 \leq t < t_o)$. L-61-2189

Figure 5.- Leading edge of gamma pulse (τ_o = 455 μsec).

using neutron excitation is shown in (Fig. 6). All pulses using neutron excitation were obtained with $\tau_o = 455$ μsec.

Observation of figures (3), (4), (5) and (6) indicates that at least two components of decay can be resolved. One can easily distinguish a fast component which lasts for approximately 100 mμsec and a longer component which dies out after about 2 μsec. There are probably longer decay components, but with available equipment these could not be resolved. The scintillation pulse shape $\gamma(t) = 1 - E(t)/E_o$ was calculated using data obtained from the leading edge of the experimentally determined voltage pulses. For this calculation, the transit time of the multiplier tube was neglected, i.e. $\delta_k = o$. The value of E_o was taken to be the maximum observable deflection of the voltage pulse. The scintillation pulse shape was plotted on semi-log paper as a function of time. Figure (7) illustrates typical scintillation pulse shapes ($\gamma(t)$ versus t) for stilbene using neutron and gamma-ray excitation.

Figure (7) clearly indicates that the scintillation pulse is composed of at least two exponential components of decay. By assuming that, for $t > 200$ mμsec, the fast component has died out and only the longer component remains, the decay parameters and the fraction of light carried by each component can be calculated. Let τ_1 and τ_2 be the decay time for the short and long components respectively. The fraction of light carried by each component is defined as $\frac{q_1}{q_o}$ and $\frac{q_2}{q_o}$. Values of these parameters were obtained for several pulses, using both gamma-ray and neutron excitation. The results of these calculations are tabulated in table I. These results agree generally with those published in references 1-6. However, no direct comparison can be made since the purity of the crystal used is not known.

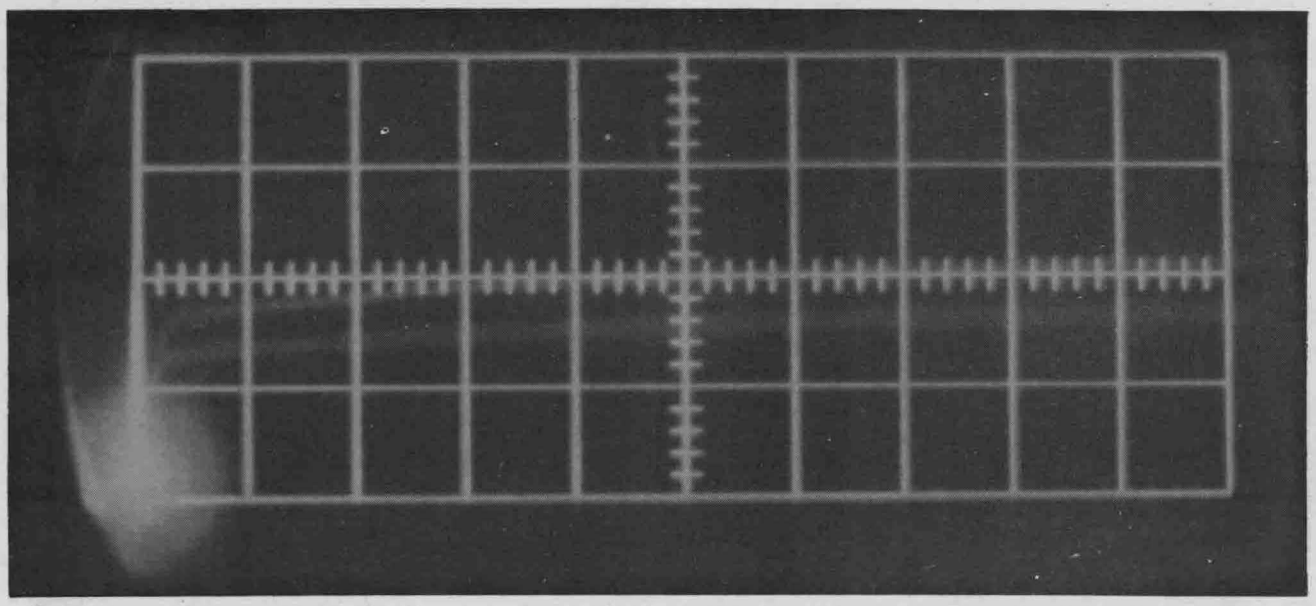

E(t) versus t $\quad (0 \leq t < t_o)$. L-61-2190

Figure 6.- Leading edge of neutron pulse (τ_o = 455 μsec).

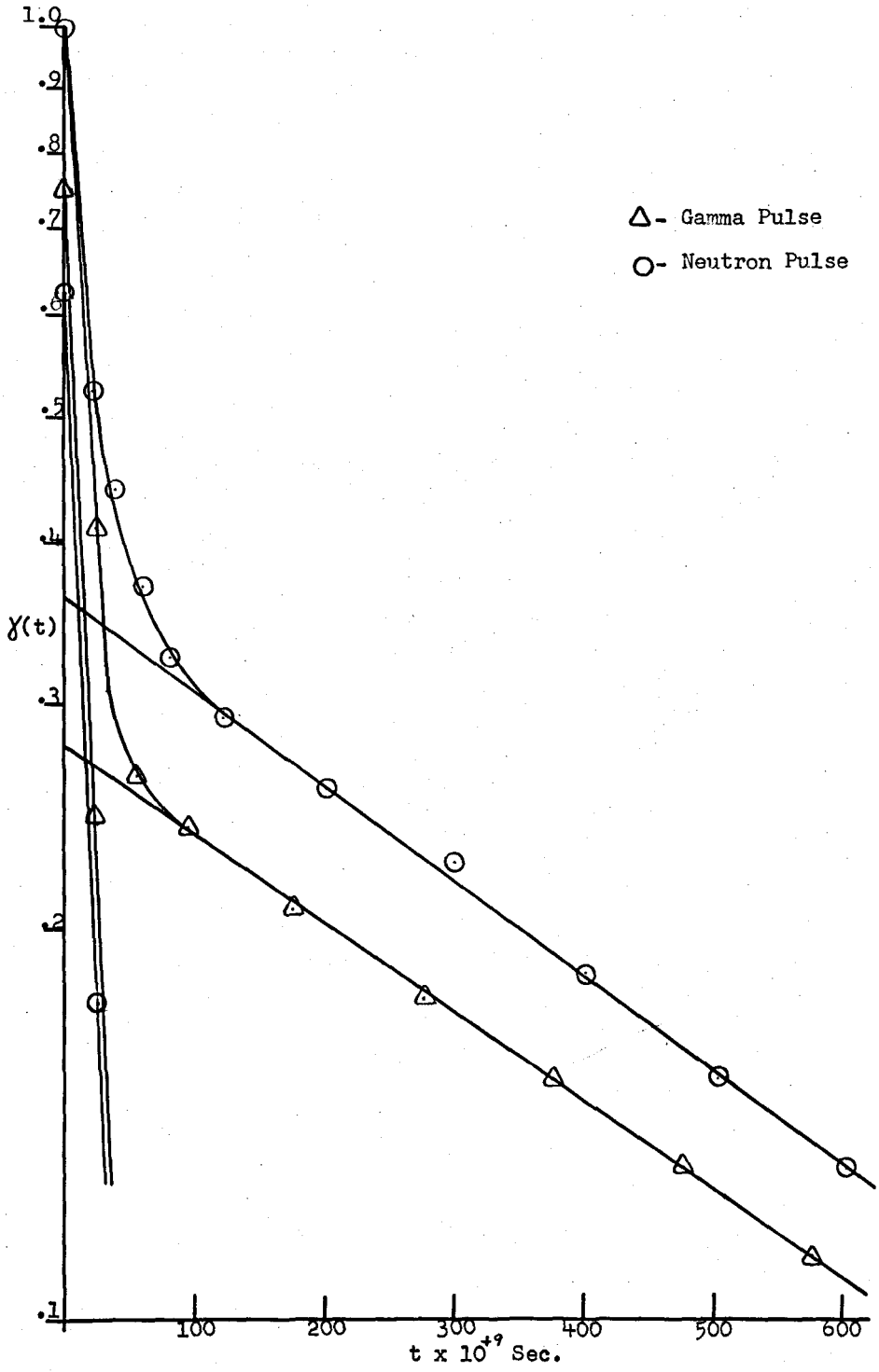

Figure 7.- Scintillation pulse shape.

TABLE I

Excitation	τ_o, μsec	E_o, volts	τ_1, mμsec	τ_2, mμsec	$\frac{q_1}{q_o}$	$\frac{q_2}{q_o}$	$\frac{q_1}{q_2}$
Gamma	91	0.170	13.9	655	0.725	0.275	2.64
	310	.175	12.8	617	.725	.275	2.64
	310	.190	14.0	614	.736	.264	2.79
	455	.260	12.2	624	.723	.277	2.61
	455	.169	13.8	647	.740	.260	2.85
Mean			13.3	631			2.71
Neutron	455	0.300	18.1	615	0.637	0.363	1.75
	455	.211	16.3	625	.660	.340	1.94
	455	.230	15.4	600	.638	.362	1.76
	455	.200	14.7	575	.690	.310	2.22
	455	.310	15.2	563	.688	.312	2.20
	455	.335	17.7	543	.650	.350	1.86
	455	.178	13.5	587	.700	.300	2.33
	455	.200	14.4	570	.638	.362	1.76
Mean			15.7	584			1.97
Overall mean			14.8	603			

VII. CONCLUSIONS

From a comparison of figure 6 and table I, it appears that the decay parameter, τ_1, is independent of the type of initial excitation. One might also conclude that the long component decay parameter, τ_2, is virtually the same for neutron and gamma excitation. Any large difference between $(\tau_2)_\gamma$ and $(\tau_2)_n$ is due to inherent errors in the measuring apparatus and in the determination of $\gamma(t)$. It is believed that the main sources of error are the finite rise time of the oscilloscope and the dispersion of the pattern obtained on the scope.

Since the decay parameters seem to be independent of the type of radiation, one infers that the modes of energy transfer and de-excitation are the same for both neutron and gamma excitation. This result is in agreement with the work of Owens. However, the results tabulated in table I indicate that the percentage light output associated with the long component is definitely larger for neutrons than for gamma-rays. This indicates that the relative number of excited molecules which decay with the large decay parameter is greater for neutron than for gamma-ray excitation.

Assuming that the observed differences in a decay parameter for different types of excitation are due only to the inability to measure them accurately, we want to show that the effective composite decay time for neutron excitation is considerably longer than for gamma-rays. This assumption is not only based on results determined here, but also in the results obtained by Owens, Brooks, Kallman and Brucker. Weighing each determination of τ_1 and τ_2 the same, regardless of type of excitation

mean values were found to be $\bar{\tau}_1 = 14.8$ mμs and $\bar{\tau}_2 = 603$ mμs.

Rewriting equation (16) for two components ($l=2$) and using mean values for τ_1 and τ_2, we obtain,

$$\frac{E(t)}{E_o} = \frac{1}{\beta + 1}\left\{\frac{\beta\tau_o}{\bar{\tau}_1 - \tau_o}\left[e^{-t/\bar{\tau}_1} - e^{-t/\tau_o}\right] + \frac{\tau_o}{\bar{\tau}_2 - \tau_o}\left[e^{-t/\bar{\tau}_2} - e^{-t/\tau_o}\right]\right\} \qquad (28)$$

where $\beta = \frac{q_1}{q_2}$.

Since $\tau_o \gg \tau_2 \gg \tau_1$ the above equation reduces to

$$\frac{E(t)}{E_o} = \frac{1}{\beta + 1}\left\{\beta\left(1 - e^{-t/\bar{\tau}_1}\right) + \left(1 - e^{-t/\bar{\tau}_2}\right)\right\} \qquad (29)$$

Since the mean values $\bar{\tau}_1$ and $\bar{\tau}_2$ do not change with type of excitation, the above equation is a function of time and β only. Differentiating equation (28) and setting the results equal to zero one can determine the time, t_o, required for the voltage pulse to reach its maximum value. Since $t_o \gg \bar{\tau}_1$, then $e^{-t_o/\bar{\tau}_1} \approx 0$,

$$t_o = \frac{\bar{\tau}_2\tau_o}{\bar{\tau}_2 - \tau_o} \ln \frac{\bar{\tau}_2}{\tau_o}\left[\beta\left(\frac{\bar{\tau}_2 - \tau_o}{\bar{\tau}_1 - \tau_o}\right) + 1\right]. \qquad (30)$$

For a fixed value of τ_o the only factor which will influence the value of t_o for different types of excitation is $\frac{q_1}{q_2} = \beta$. For $\tau_o \gg \tau_2 \gg \tau_1$ the above equation reduces to

$$t_o = -\bar{\tau}_2 \ln \frac{\bar{\tau}_2}{\tau_o}\left[\beta + 1\right] \qquad (31)$$

The effective difference in duration of the leading edge of pulse produced by neutrons and gamma-rays is given by

$$\Delta t_o = (t_o)_n - (t_o)_\gamma = -\bar{\tau}_2 \ln \frac{\bar{\tau}_2}{\tau_o}\left[\beta_n + 1\right] - \bar{\tau}_2 \ln \frac{\bar{\tau}_2}{\tau_o}\left[\beta_\gamma + 1\right]$$

$$= -\bar{\tau}_2 \ln \left[\frac{\beta_n + 1}{\beta_\gamma + 1}\right] \qquad (32)$$

It is important to note that Δt_o depends only on $\bar{\tau}_2$ and the values of β_n and β_γ. Using the values of $\bar{\tau}_2$, β_n and β_γ determined experimentally (table I), Δt_o is found to be 140 μsec.

Thus, the above result indicates that a neutron pulse has a longer effective decay time than the corresponding gamma pulse. The plot of equation (29) using appropriate values of β, is illustrated in figure 8. The effective decay time difference between the leading edges of neutron and gamma pulses can easily be seen. Figure 8 indicates that the neutron pulse actually lags behind the gamma pulse by 140 μsec. The reason for this effective decay time difference is that a neutron scintillation contains a larger proportion of slow components than a gamma scintillation, each having the same total light in the scintillation. In accordance with equation (32), a decay time difference will always exist, except for $\beta_n = \beta_\gamma$. It was found without exception in this experiment that $\beta_\gamma > \beta_n$, thus indicating a definite decay difference.

The results of this experiment indicate that for neutron excitation more light is emitted in the slow component of the scintillation than for gamma excitation, i.e. $\left(\frac{q_2}{q_o}\right)_n > \left(\frac{q_2}{q_o}\right)_\gamma$. Also it was found that $\left(\frac{q_1}{q_2}\right)_n < \left(\frac{q_1}{q_2}\right)_\gamma$

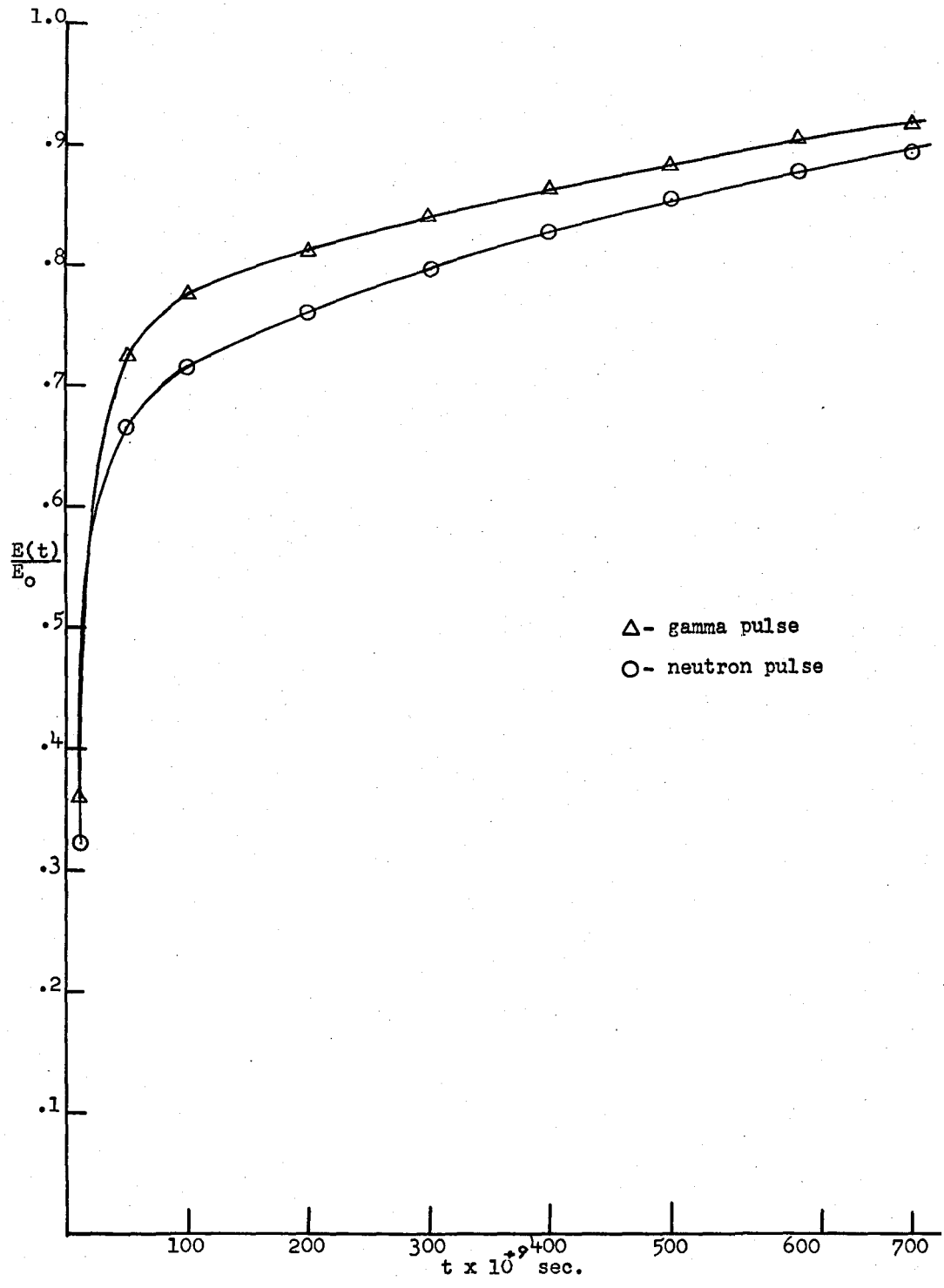

Figure 8.- Leading edge of voltage pulse.

since more of the light emitted in the fast component is quenched in the case of neutron excitation. In order for the explanation given in the introduction to accurately describe the effective decay time difference, the above two results must be valid[5]. In this experiment both of the above conditions were experimentally verified, thus supporting previous analysis.

VIII. ACKNOWLEDGEMENTS

The author wishes to express his appreciation to Dr. Addison D. Campbell for his advice, direction, and encouragement throughout the entirety of this investigation; also to Dr. B. W. Sloope and Mr. J. J. Taylor; and to his wife, Barbara, whose faith and patience never waned.

IX. BIBLIOGRAPHY

1. Sharpe, J.: Nuclear Radiation Detectors, (Wiley and Sons), pp. 27-46.
2. Birks, J. B.: Scintillation Counters, (Pergamon Press), pp. 1-36.
3. Brooks, F. D.: Progress in Nuclear Physics 5, 1956, pp. 230-260.
4. Wright, G. T.: Proc. Phys. Soc. (London) B69, pp. 358-372.
5. Brooks, F. D.: Nuclear Instr. 4, 1959, pp. 151-163.
6. Owens, R. B.: United Kingdom Atomic Energy Research Establishment Report EL/R 2712, Harwell, 1958.
7. Broek, H. W., and Anderson, C. E.: Review Scientific Instruments, 31, 1960, pp. 1063-1069.
8. Funsten and Cobb: Review of Scientific Instruments, May 1960.
9. Phillips, H. B., and Swank, R. K.: Rev. Sci. Instr. 24 (1953) 611.
10. Swank, R. K., and Buck, R. W.: Rev. Sci. Instr. 26 (1955) 15.
11. Harrison, F. B.: Nucleonics 12, No. 3 (1954) 24; Phys. Rev. 89 (1953) 322.
12. Birks, J. B.: Proc. Phys. Soc., A64 (1951) p. 874.
13. Kallmann, H., and Brucker, G. J.: Phys. Rev. 108 (1957) p. 1122.